

Prediction of aftershocks with Gaussian process regression

Kosuke Morikawa¹, Hiromichi Nagao^{2,3}, Shin-ichi Ito^{2,3}, Yoshikazu Terada^{1,4},
Shin'ichi Sakai^{2,5} and Naoshi Hirata^{2,6}.

¹ *Graduate School of Engineering Science, Osaka University, 1-3, Machikaneyama-cho, Toyonaka-shi, Osaka 5608531, Japan.*

² *Earthquake Research Institute, The University of Tokyo, 1-1-1, Yayoi, Bunkyo-ku, Tokyo 113-0032, Japan.*

³ *Graduate School of Information Science and Technology, The University of Tokyo, 7-3-1, Hongo, Bunkyo-ku, Tokyo 113-8656, Japan.*

⁴ *Center for Advanced Intelligence Project, RIKEN, 1-4-1, Nihonbashi, Chuo-ku, Tokyo 103-0027, Japan.*

⁵ *Interfaculty Initiative in Information Studies Graduate School of Interdisciplinary Information Studies, The University of Tokyo, 7-3-1, Hongo, Bunkyo-ku, Tokyo 113-0033, Japan.*

⁶ *National Research Institute for Earth Science and Disaster Resilience, 3-1, Tennodai, Tsukuba-shi, Ibaraki 305-0006, Japan.*

SUMMARY

Uncovering the distribution of magnitudes and arrival times of aftershocks is a key to comprehend the characteristics of the sequence of earthquakes, which enables us to predict seismic activities and hazard assessments. However, identifying the number of aftershocks is very difficult due to contaminations of arriving seismic waves immediately after the main shock. To overcome the difficulty, we construct a likelihood based on the detected data incorporating a detection function to which the Gaussian process regression (GPR) is applied. The GPR is capable of estimating not only the parameter of the distribution of aftershocks together with the detection function, but also credible intervals

for both of the parameters and the detection function. A property of both the Gaussian process and a distribution of aftershocks are exponential functions leads to an efficient Bayesian computational algorithm to estimate the hyperparameters. After the validations through numerical tests, the proposed method is retrospectively applied to the catalog data related to the 2004 Chuetsu earthquake towards early forecasting of the aftershocks. The result shows that the proposed method stably estimates the parameters of the distribution simultaneously their uncertainties even within three hours after the main shock.

Key words: Aftershock distribution; detection function; point process; Gaussian process regression.

1 INTRODUCTION

A large earthquake triggers a number of aftershocks. There have been proposed reasonable models to describe the distribution of aftershocks with temporal information as well as magnitudes such as the Omori-Utsu (Omori 1894; Utsu 1961) and the Gutenberg-Richter (Gutenberg & Richter 1944) formulae. The distribution of aftershocks enables us to forecast seismic activities and hazard assessments (Resenberg & Jones 1989, 1994; Kagan & Jackson 2000). Until now, many statistical methods to estimate parameters involved in the models have been proposed (Aki 1965; Ogata 1983). The disadvantages in these methods are that they assume the existence of complete data without missing, though detecting all aftershocks immediately after the main shock is impossible due to contaminations of a tremendous amount of seismic waves. Such incomplete data cause underestimations in the counting of aftershocks.

In statistics, situations only some detected data being available are known as biased sampling problem (Vardi 1982, 1985). In our case, detection probability of aftershocks clearly depends on the magnitudes and elapsed times from the main shock. This type of biased sampling data is known as missing not at random (MNAR), in which the detection probability depends on the values of undetected data. Introducing a detection function, which is a model of the detection probability, enables us to correct the bias (Qin 2017). Several studies have tackled this problem by introducing a parametric model on the detection function for aftershocks (Ringdal 1975; Ogata & Katsura 1993, 2006; Omi et al. 2013, 2014, 2015a,b). The detection function enables us to construct valid estimators in MNAR. Three problems remain to be solved: (i) the resulting estimators are often unstable; (ii) misspecification of the detection function causes bias; (iii) estimation of the detection function is difficult even with a correct model. The first problem (i) arises from the simultaneous estimation of the detection func-

tion and the distribution of aftershocks. The second problem (ii) is obvious because the bias correction strongly depends on how close the defined detection function to the true one is. The third problem (iii) is because some integration is required in the likelihood, which makes estimations difficult in biased sampling problems.

In this study, we propose a nonparametric Bayesian estimator to overcome all the three problems. Appropriate prior information considering characteristics of seismic activities in a target area improves the first problem (i). A technique of Gaussian process regression (GPR), which is nonparametric Bayesian estimation, models the detection function, simultaneously solving the problems (i) and (ii). Owing to the nonparametric modeling, the detection function does not need to have a specific functional form. The GPR has been often used especially in the recent machine learning and deep learning researches due to its flexibility and wide coverage of function spaces (Rasmussen et al. 2006; de G. Matthews et al. 2018). As for computation of the model parameters, we propose an efficient Bayesian estimation algorithm utilizing the property that both the GP and the distribution of aftershocks are exponential functions, which are compatible to compute solving the third problem (iii).

Another advantage in GPR is that it is capable of evaluating uncertainty of the estimated parameters naturally, which has been hard in the previous works though knowing the uncertainty is inevitable to decide statistical decision. In summary, the proposed method can solve the three problems and has an additional property that can estimate the uncertainty of the parameters.

This paper is organized as follows. Section 2 introduces the GPR, and proposes a method to estimate parameters for distribution of aftershocks with a detection function through the GPR. Section 3 validates the proposed method through numerical tests. Section 4 demonstrates the effectiveness of the proposed method by applying to the catalog data of 2004 Chuetsu earthquake. Section 5 concludes the present study including perspective future works.

2 METHODOLOGY

The detection function proposed in this paper that models temporal changes of the detection rate of the aftershocks right after a main shock bases GPR. This section gives first a brief explanation related to the GPR, then introduces the proposed method especially its theoretical properties and an efficient computational algorithm.

2.1 Gaussian process regression

Some recent studies in the solid Earth science used the GPR to construct models from given data in the cases that the physical or chemical process that produced the data was unknown or too compli-

cated. The GPR estimates a regression function simultaneously with its uncertainty through Bayesian nonparametric estimation. For example, Kuwatani et al. (2018) proposed to apply the GPR to interpolate the observed quantities of chemical compositions along with the radius of a rock. The estimated uncertainty often provides valuable information for observational or experimental design, such as a suggestion of times and/or places of the next new observations or measurements.

In this study, GPR is used as a tool for Bayesian nonparametric estimation for a regression function. Let $\mathbf{x} = (x_1, \dots, x_n)^\top$ and $\mathbf{y} = (y_1, \dots, y_n)^\top$ be sets of explanatory and response variables, respectively, and both are assumed to relate each other through an unknown regression function $f(\cdot)$, i.e., $y_i = f(x_i)$ ($i = 1, \dots, n$), where n denotes the number of time points. In this paper, we use the notation like $f(\cdot)$ to abbreviate the arguments by a dot emphasizing that f is a function. The GPR estimates the function $f(\cdot)$ from the given a dataset assuming a kernel function mentioned below. In probability theory and statistics, a Gaussian process (GP) is a stochastic process such that every finite collection of those random variables has a multivariate normal distribution, e.g. $\mathbf{f} = (f(x_1), \dots, f(x_n))$ follows a multivariate normal distribution. One can think of the GP as defining a distribution over functions for a target function that promotes effective Bayesian estimation giving a priori information of the function (Rasmussen et al. 2006). The GP is usually denoted as $\text{GP}(f_0(\cdot), \mathcal{K}(\cdot, \cdot))$, where $f_0(\cdot)$ is mean function and $\mathcal{K}(\cdot, \cdot)$ is variance function or ‘‘kernel’’. The mean function $f_0(\cdot)$ is often assumed as identically zero since the mean is adjustable by subtracting the sample mean of \mathbf{y} . The radial basis function is often chosen among various candidate functions for the variance function or kernel $\mathcal{K}(\cdot, \cdot)$:

$$\mathcal{K}(x_1, x_2) = \phi_1 \exp \left\{ -\frac{(x_1 - x_2)^2}{\phi_2^2} \right\} \quad (\phi_1, \phi_2 > 0), \quad (1)$$

where x_1 and x_2 are arbitrary real numbers. This study also adopts the radial basis function for the kernel since it adequately covers an infinite-dimensional function space of $\mu(\cdot)$ with only a few hyperparameters. See Rasmussen et al. (2006) for the detailed explanation of GP including other kernel functions.

Estimation of a function $f(\cdot)$ is equivalent to that of the value of $f(x^*)$ at any fixed point x^* , where the superscript ‘‘*’’ is used to discriminate the fixed point from the data points. For any point x^* a posterior distribution of $f^* = f(x^*)$ given a dataset $\mathcal{D} = \{x_1, \dots, x_n, y_1, \dots, y_n\}$ is called the predictive distribution. By using the Bayes’ theorem, calculation of the predictive distribution is given by

$$p(f^* | x^*, \mathcal{D}) = \int p(f^* | x^*, \mathbf{f}, \mathcal{D}) p(\mathbf{f} | \mathcal{D}) d\mathbf{f}, \quad (2)$$

where $p(f^* | x^*, \mathbf{f}, \mathcal{D})$ and $p(\mathbf{f} | \mathcal{D})$ are the conditional probability density function (PDF) of f^* given the fixed point x^* , unobserved \mathbf{f} , and the dataset \mathcal{D} . The PDF $p(\mathbf{f} | \mathcal{D})$ is the prior on \mathbf{f} given by a multivariate normal distribution as mentioned above. In this case, the predictive distribution can

be explicitly obtained and becomes a normal distribution again because both $p(f^* | x^*, \mathbf{f}, \mathcal{D})$ and $p(\mathbf{f} | \mathcal{D})$ are normal distributions. Therefore, the predictive distribution for a point x^* is a normal distribution with mean $\mu_f(x^*)$ and variance $\sigma_f^2(x^*)$ computed as

$$\mu_f(x^*) = \kappa_*^\top \mathcal{K}^{-1} \mathbf{y}, \quad \sigma_f^2(x^*) = \kappa_{**} - \kappa_*^\top \mathcal{K}^{-1} \kappa_*,$$

where $\kappa_* = \{\mathcal{K}(x^*, x_1), \dots, \mathcal{K}(x^*, x_n)\}^\top$ and $\kappa_{**} = \mathcal{K}(x^*, x^*)$. The maximization of the marginal likelihood

$$\prod_{i=1}^n p(y_i | x_i; \phi) = \prod_{i=1}^n \int p(y_i | x_i, \mathbf{f}; \phi) p(\mathbf{f} | x_i; \phi) d\mathbf{f}. \quad (3)$$

determines the hyperparameters $\phi = (\phi_1, \phi_2)$, where the integration in the right-hand side is explicitly computable since the integrand given as the product of normal distributions $p(y_i | x_i, \mathbf{f}; \phi)$ and $p(\mathbf{f} | x_i; \phi)$ is again a normal distribution.

Figure 1 shows the estimated predictive distributions from six data points with changing hyperparameters ϕ_1 and ϕ_2 in the kernel (eq. 1). As mentioned above, the GPR successfully obtains not only the mean function but also its standard error or credibility. Figure 1 also indicates ϕ_1 and ϕ_2 strongly associate with scale and shape of the regression function, respectively. A comparison between Figures 1(a) and 1(c), or 1(b) and 1(d) indicates that small/large ϕ_1 means a small large/credible interval. Another comparison between Figure 1(a) and 1(b), or 1(c) and 1(d) shows that small/large ϕ_2 means an oscillating/smoothed regression function. These results indicate the importance of deciding the hyperparameters.

2.2 Notation and models

According to the Omori-Utsu law, aftershock occurrence rate $n(t)$ at elapsed time t from the main shock follows a non-stationary Poisson process (Omori 1894; Utsu 1961):

$$n(t; \boldsymbol{\tau}) = \frac{K}{(t+c)^p},$$

where $\boldsymbol{\tau}$ is a vector containing all the model parameters, i.e., $\boldsymbol{\tau} = (K, p, c)^\top$. The parameter K controls the level of seismic activity, i.e., large/small K reflects the large/small number of aftershocks. The parameter p is the slope of the occurrence rate in the logarithmic scale. It is known that the occurrence rate is saturated over a period of time right after the main shock (Utsu 1961; Ogata 1983), and the parameter c determines the time length of the saturation. According to the Gutenberg-Richter's law, intensity rate of the magnitude M is modeled as a function proportional to an exponential function (Gutenberg & Richter 1944):

$$m(M; b) = A10^{-bM} \propto \exp(-\beta M), \quad (4)$$

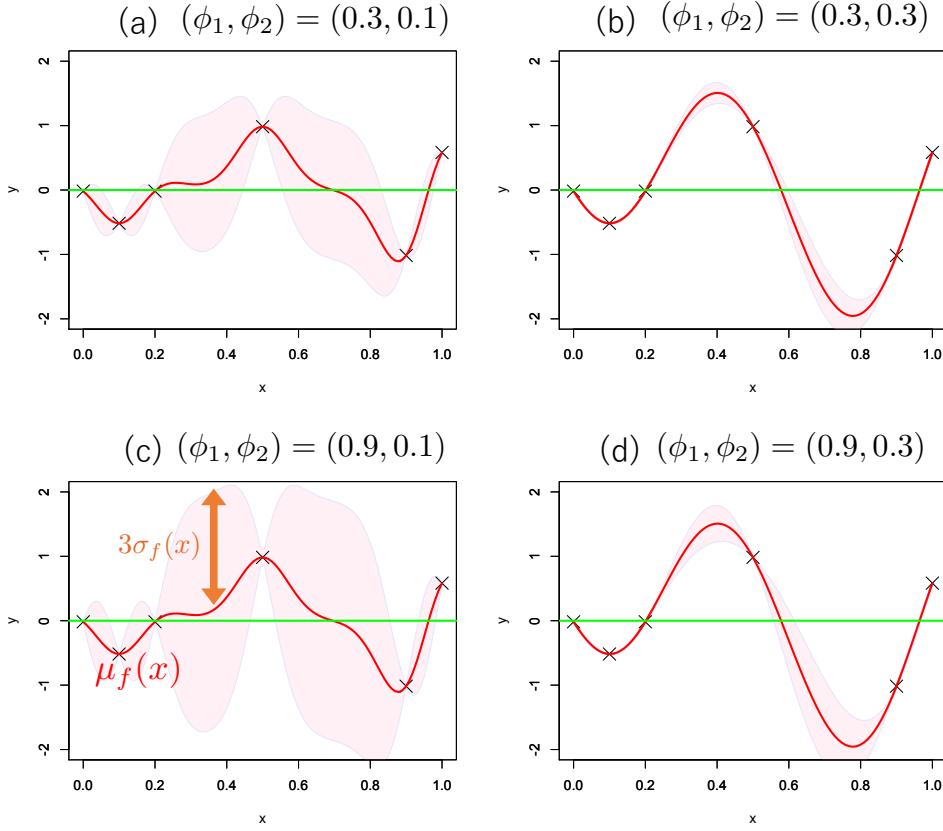


Figure 1. Gaussian process regression applied to six data points (“ \times ”) with different hyperparameters (ϕ_1, ϕ_2) . The green line is the mean function $f_0(\cdot)$ of the prior distribution, which is assumed to be identically zero, the red curve is the estimated mean $\mu_f(\cdot)$ of the predictive distribution, and shaded region is the deviation $3\sigma_f(\cdot)$ from the mean of the predictive distribution.

where A is a constant, and b (or $\beta = b \ln 10$), which is of our most interest, controls the amplitude of the magnitudes. Combining these two laws, the joint occurrence rate of aftershocks as a function of elapsed time t and magnitude M is represented by the product of $n(t)$ and $m(M)$ as

$$\lambda(t, M; \boldsymbol{\tau}, \beta) = \frac{K'}{(t+c)^p} \beta e^{-\beta(M-M_0)}, \quad (5)$$

where $K' = \beta^{-1}KA \exp(-\beta M_0)$ and M_0 is the magnitude of the main shock used to adjust the scale of K' (Utsu 1970). Note that even if K' is obtained, K can not be uniquely identified due to the unidentifiability of the product KA . Resenberg & Jones (1989, 1994) found that estimation of K' enables us to forecast seismic activities, so that the identifiability problem does not matter in this context. Hereafter we use K instead of K' for notational simplicity.

An exact count of all aftershocks right after a main shock is very difficult due to contaminations of arriving seismic waves, so that the occurrence rate of aftershocks are almost always underestimated. In

order to correct the bias, the present study adopts probit-type detection function as is used in Ringdal (1975), Ogata & Katsura (1993), Ogata & Katsura (2006), and Omi et al. (2013, 2014, 2015a,b):

$$\begin{aligned}\pi(t, M; \mu, s) &= P(\delta = 1 | t, M; \mu, s) \\ &= \int_{-\infty}^M \frac{1}{\sqrt{2\pi s^2}} \exp \left\{ -\frac{(x - \mu(t))^2}{2s^2} \right\} dx,\end{aligned}\quad (6)$$

where δ is a detection indicator that takes 1/0 if the aftershock is detected/undetected, $\mu(t)$ is the magnitude that makes aftershock detectable with probability 50% at elapsed time t , and s is a scale parameter. Roughly speaking, the function $\mu(t)$ is decreasing with respect to the elapsed time t because only large aftershocks are detectable immediately after the main shock and even small aftershocks are detectable after enough time passes.

To make the difference between complete and detected data clear, let each t_1 and M_1 be the elapsed time and magnitude of a detected aftershock, respectively. The subscript “1” indicates the detected data, i.e., $\delta = 1$. Note that, in this study, complete data t and M might not be detected, but t_1 and M_1 are always available. Supposing that n aftershocks are detected, let the pair of elapsed time from the main shock and magnitude of i -th aftershock be (t_{1i}, M_{1i}) ($i = 1, \dots, n$). By using technique of the thinning operation or the random deletion in point processes (Ogata & Katsura 1993), the likelihood function for the detected magnitudes can be written by

$$\begin{aligned}& \prod_{i=1}^n L(M_{1i} | t_{1i}; \beta, \mu, s^2) \\ &= \prod_{i=1}^n \frac{e^{-\beta M_{1i}} \pi(t_{1i}, M_{1i}; \mu, s^2)}{\int_{-\infty}^{\infty} e^{-\beta M} \pi(t_{1i}, M; \mu, s^2) dM} \\ &= \prod_{i=1}^n \beta \exp \left\{ -\beta(M_{1i} - \mu(t_{1i})) - \frac{1}{2}\beta^2 s^2 \right\} \pi(t_{1i}, M_{1i}; \mu, s^2),\end{aligned}\quad (7)$$

where the function $\mu(\cdot)$ is assumed to be known, although it is estimated later in practice. Let $\hat{\beta}$ and \hat{s} be the estimated values for β and s obtained by maximizing the likelihood. With estimated $\hat{\beta}$ and \hat{s} , τ can be estimated by maximizing the log-likelihood function for detected elapsed times within any time interval $(0, T)$ (Ogata & Katsura 1993),

$$\sum_{0 < t_{1i} < T} \ln \nu(t_{1i}; \tau, \hat{\beta}, \hat{s}) - \int_0^T \nu(t; \tau, \hat{\beta}, \hat{s}) dt,\quad (8)$$

where $\nu(t)$ is an intensity function for detected data defined by

$$\begin{aligned}\nu(t; \tau, \beta, s) &= \int_{-\infty}^{\infty} \lambda(t, M; \tau, \beta) \pi(t, M; s) dM\end{aligned}\quad (9)$$

$$= \frac{K}{(t+c)^p} \exp \left\{ -\beta(\mu(t) - M_0) + \frac{1}{2}\beta^2 s^2 \right\}.\quad (10)$$

This paper proposes a more efficient estimation method for τ in Section 2.4, obtained from an investigation of the problem in the estimations of β and s as mentioned in Section 2.3.

However, it remains one serious problem that $\mu(\cdot)$ is unknown. In frequentist ways, Ogata & Katsura (1993) applied a B-spline basis function to $\mu(\cdot)$, and Ogata & Katsura (2006) proposed a specific parametric model based on the 2003 Miyagi-Ken-Oki earthquake as

$$\mu(t) = a_0 + a_1 \exp\{-\alpha(3 + \ln t)^\gamma\},$$

where a_0 , a_1 , α , and γ are parameters to be estimated. Recently, Omi et al. (2013) proposed a flexible nonparametric Bayesian estimation. They assumed a prior on $\mu(t_{1i})$ ($i = 1, \dots, n$), and compute the posterior mean. Their method does not require any specification of $\mu(\cdot)$ and, because of Bayesian estimation, it can naturally incorporate the prior information of β , which considerably makes estimates stable. The distribution of β can be easily computed in the same area before the main shock. However, it is hard to estimate credibility of neither $\mu(t_{1i})$ ($i = 1, \dots, n$) nor β by their method. Estimating the credibility of the estimator is inevitable to decide statistical decision.

2.3 Estimation for β , s^2 , and $\pi(\cdot)$

In this study, we put a Gaussian process (GP) prior on the “function” $\mu(\cdot)$, not on the “points” $\mu(t_{1i})$ ($i = 1, \dots, n$). The GP prior leads to an explicit form of the marginal likelihood of hyperparameters and posterior distribution of $\mu(\cdot)$ as seen in the following discussion.

A graphical model for complete data is shown at the left panel in Figure 2. The graphical model illustrates the relations among data, parameters, and hyperparameters in accordance with Omori-Utsu and Gutenberg-Richters laws and the detection function, which enables us to grasp the notation and models in this study. Each green, red, blue color indicates the relation by Omori-Utsu law, Gutenberg-Richter’s law, and the detection function, respectively. To avoid the problem, we focus on the partial likelihood, which is the distribution of detected magnitude M_1 given t_1 , derived in eq. (7). Once the graphical model for the detected data was obtained, one would realize that relation among M_1 , μ , and t_1 is exactly the same as the regression. Based on this idea, we put a Gaussian process prior on $\mu(\cdot)$, that corresponds to $f(\cdot)$ in Section 2.1, and consider nonparametric bayesian estimation. However, unlike the GPR explained in Section 2.1, the distribution (eq. 7) is not a normal distribution, and the predictive distribution shall be more complicated.

The Gaussian process assumption on $\mu(\cdot)$ is denoted by $\mu \sim \text{GP}(\mu_0(\cdot), \mathcal{K}(\cdot, \cdot))$, where \mathcal{K} is defined as

$$\mathcal{K}(x_1, x_2) = \phi_0 + \phi_1 \exp\left\{-\frac{(x_1 - x_2)^2}{\phi_2^2}\right\} \quad (\phi_1, \phi_2 > 0).$$

As for $\mu_0(\cdot)$, some reasonable function should be chosen because adjusting the mean of the prior

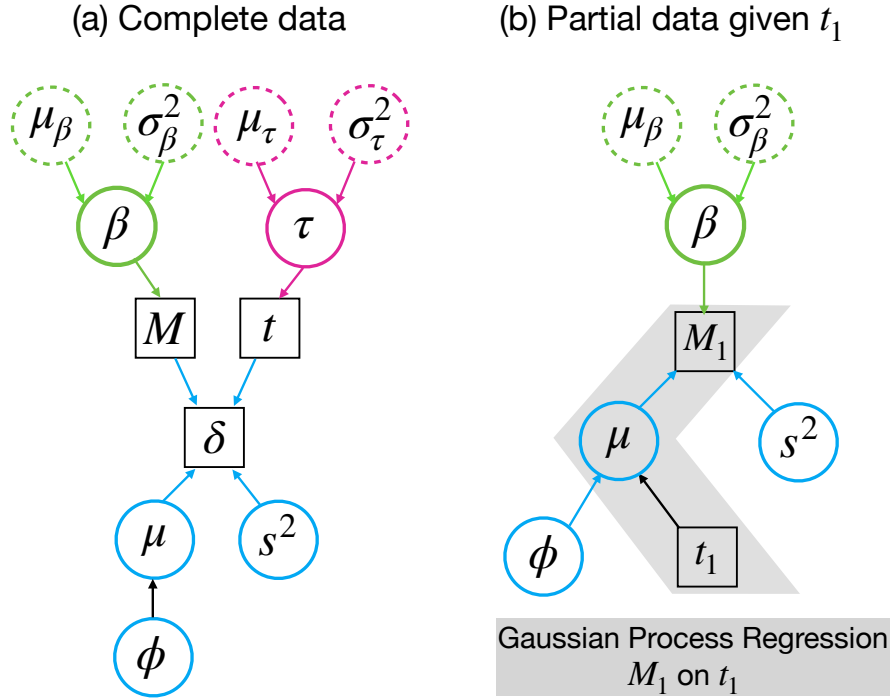


Figure 2. Graphical models on (a) complete data; (b): partial or detected data given t_1 . Each square, circle, and dotted circle indicates data, parameters, and subjective hyperparameters, respectively.

$\mu_0(\cdot)$ to identically zero is impossible unlike the usual GPR. In this paper, a simple linear model $\mu_0(t_{1i}) = a_0 + a_1 t_{1i}$ is used as the mean of the prior distribution. The unknown parameters a_0 and a_1 are estimated by maximizing eq. (7) with the simple linear model. It can be seen later that this simple prior works well in the numerical experiments in Section 3. One difference between the above kernel and eq. (1) is the first term ϕ_0 . This term prevents \mathcal{K}^{-1} from being a nonsingular matrix and is set very small value (e.g. 10^{-7}) so that it does not affect estimation of the other parameters. The additional parameters to be estimated are only ϕ_1 and ϕ_2 , so that the remaining parameters are $\theta = (\beta, s^2, \phi_1, \phi_2)$. Let $\theta_0 = (\mu_\beta, \sigma_\beta^2)$ be the known parameters prescribing the distribution of θ , i.e. subjective priors.

Predictive distribution of $\mu(\cdot)$ and the marginal likelihood of the hyperparameters are computable as follows. The proof is relegated to the Appendix.

- Marginal likelihood of $\boldsymbol{\theta} = (\beta, s^2, \phi_1, \phi_2)$:

$$\begin{aligned}
& p(\mathcal{D} \mid \boldsymbol{\theta}) \\
&= p(\boldsymbol{\theta}; \boldsymbol{\theta}_0) \int p(\mathbf{M}_1 \mid \mathbf{t}_1; \beta, \boldsymbol{\mu}, s^2) p(\boldsymbol{\mu} \mid \mathbf{t}_1; \phi_1, \phi_2) d\boldsymbol{\mu} \\
&= \beta^n \exp \left\{ -\beta \sum_{i=1}^n (M_{1i} - \mu_{0,i}) - \frac{1}{2} \beta^2 \left(ns^2 - \sum_{i,j} \mathcal{K}_{i,j} \right) \right\} \\
&\quad \times p(\boldsymbol{\theta}; \boldsymbol{\theta}_0) \int_{\mathcal{M}} \mathcal{N}(\mathbf{x}; \tilde{\boldsymbol{\mu}}, \tilde{\mathcal{K}}) d\mathbf{x}, \tag{11}
\end{aligned}$$

where $\mathbf{t}_1 = (t_{11}, \dots, t_{1n})^\top$, $\mathbf{M}_1 = (M_{11}, \dots, M_{1n})^\top$, $\mathcal{M} = \otimes_{i=1}^n \{x_i \leq M_{1i}\}$ is the integration interval, $\tilde{\boldsymbol{\mu}} = \boldsymbol{\mu}_0 + \beta K \mathbf{1}$, $\tilde{\mathcal{K}} = \mathcal{K} + s^2 I_n$, I_n is the n by n identity matrix, and $\mathcal{N}(\mathbf{x}; \boldsymbol{\mu}, \Sigma)$ is density function of the normal distribution with mean $\boldsymbol{\mu}$ and variance Σ .

- Predictive distribution of $\mu(\cdot)$:

$$\begin{aligned}
& p(\mu^* \mid t_1^*, \mathcal{D}) \\
&= \int p(\mu^* \mid t_1^*, \boldsymbol{\mu}, \mathcal{D}) p(\boldsymbol{\mu} \mid \mathcal{D}) d\boldsymbol{\mu} \\
&= \mathbb{E}_{\text{trunc}} \left\{ \mathcal{N}(\mu^*; D^*(\mathbf{X}), (\tau^*)^2) \right\}, \tag{12}
\end{aligned}$$

where $\mathbb{E}_{\text{trunc}}$ is expectation on a variable $\mathbf{X} \sim \mathcal{TN}(\tilde{\boldsymbol{\mu}}, \tilde{\mathcal{K}}, \mathcal{M})$, $\mathcal{TN}(\boldsymbol{\mu}, \Sigma, \mathcal{R})$ is the multivariate normal distribution with mean $\boldsymbol{\mu}$, variance $\tilde{\mathcal{K}}$, and truncated outside a region \mathcal{R} ,

$$D^*(\mathbf{x}) = (\mathbf{x} + s^2 \mathcal{K}^{-1} \tilde{\boldsymbol{\mu}})^\top \left\{ \tau^2 \tilde{\mathcal{K}}^{-1} + \tilde{\mathcal{K}}^{-1} \boldsymbol{\kappa}_* \boldsymbol{\kappa}_*^\top \tilde{\mathcal{K}}^{-1} \right\} \frac{\boldsymbol{\kappa}_*}{\boldsymbol{\kappa}_{**}},$$

$\boldsymbol{\kappa}_* = (\mathcal{K}(t_1^*, t_1), \dots, \mathcal{K}(t_1^*, t_n))^\top$, $\boldsymbol{\kappa}_{**} = \mathcal{K}(t_1^*, t_1^*)$, and $\tau^2 = \boldsymbol{\kappa}_{**} - \boldsymbol{\kappa}_*^\top \tilde{\mathcal{K}}^{-1} \boldsymbol{\kappa}_*$. In particular, mean and variance of the predictive distribution are $D^*(\boldsymbol{\xi})$ and $(\tau^*)^2$, where $\boldsymbol{\xi} = \mathbb{E}_{\text{trunc}}(X)$. The symbol “*” is used to explicitly represent that the variable depends on the value t_1^* .

- Predictive distribution of detection probability $\pi(\cdot)$:

$$\begin{aligned}
& \pi^*(M_1^*, t_1^*) \\
&= \int P(\delta = 1 \mid M_1^*, \mu^*, \mathcal{D}) p(\mu^* \mid t_1^*, \mathcal{D}) d\mu^* \\
&= \mathbb{E}_{\text{trunc}} \left\{ \Psi \left(\frac{M_1^* - D^*(\mathbf{X})}{\sqrt{s^2 + (\tau^*)^2}} \right) \right\}, \tag{13}
\end{aligned}$$

where $\Psi(\cdot)$ is the cumulant distribution function of the standard normal distribution.

Although both the marginal likelihood and the predictive distribution include integration, the integration can be regarded as expectation on some truncated multivariate normal distribution. This property is very important, and it reminds us to come up with the following computational algorithm to obtain the posterior samples of $\boldsymbol{\theta}$.

2.4 Estimation for τ

Recall that the log-likelihood function for τ is given in eq. (8), but $\pi(\cdot)$ is unknown. One possible way, as in the previous studies (Ogata & Katsura 1993; Omi et al. 2013), is replacing β , s^2 , and $\mu(\cdot)$ with estimated one. However, we now have obtained a predictive distribution of the detection function itself as given in eq. (12). Therefore, it is possible to replace the detection function (eq. 9) with the predictive one, and expected this new approach provides more efficient estimates since it uses full information of the estimated detection function, while the previous method uses only information of $\mu(\cdot)$.

By replacing the detection function (eq. 9) with the predictive one, we have

$$\begin{aligned}
 \nu^*(t; \tau, \beta, s) &= \int_{-\infty}^{\infty} \lambda(t, M; \tau, \beta) \pi^*(t, M; s) dM \\
 &= \frac{K}{(t+c)^p} \exp \left\{ \beta M_0 + \frac{1}{2} \beta^2 (s^2 + (\tau^*)^2) \right\} \\
 &\quad \times \mathbb{E}_{\text{trunc}} [\exp \{-\beta(D^*(\mathbf{X}))\}].
 \end{aligned} \tag{14}$$

The known truncated multivariate normal distribution $\mathcal{TN}(\tilde{\boldsymbol{\mu}}, \tilde{\mathcal{K}}, \mathcal{M})$ makes it possible to approximate the computation of the expectation $\mathbb{E}_{\text{trunc}}[\cdot]$ with the Monte Carol method. As for integration on t in eq. (8), we use a left Riemann sum with B , e.g. $B = 10^4$, rectangles of equal width.

2.5 Computational algorithm

Both the predictive distribution and the marginal likelihood involve integration on multivariate normal distribution over an n -dimensional hyperrectangle \mathcal{M} . It is known that explicit computation of the integral is very hard even when the dimension is low (Genz & Bretz 2009). We divide the estimation into two parts: (i) estimation of hyperparameters $\boldsymbol{\theta}$; (ii) computation of mean and variance of the predictive distribution.

We first propose a sampling method to obtain from the posterior distribution of $\boldsymbol{\theta}$ by using the data-augmentation method (Tanner & Wong 1987). Regarding a variable \mathbf{x} in eq. (11) as latent variables leads to another representation of the marginal likelihood

$$p(\mathcal{D} | \boldsymbol{\theta}) = \int_{\mathcal{M}} p(\mathcal{D}, \mathbf{x} | \boldsymbol{\theta}) d\mathbf{x},$$

where

$$\begin{aligned}
& p(\mathcal{D}, \mathbf{x} \mid \boldsymbol{\theta}) \\
&= \beta^n \exp \left\{ -\beta \sum_{i=1}^n (M_{1i} - \mu_{0,i}) - \frac{1}{2} \beta^2 \left(ns^2 - \sum_{i,j} \mathcal{K}_{i,j} \right) \right\} \\
&\quad \times \mathcal{N}(\mathbf{x}; \tilde{\boldsymbol{\mu}}, \tilde{\mathcal{K}}).
\end{aligned}$$

With the idea of Gibbs sampling, augmented data can be sampled from following two steps:

- (i) Draw $\mathbf{x} \sim p(\mathbf{x} \mid \boldsymbol{\theta}, \mathcal{D}) = \mathcal{TN}(\mathbf{x}; \tilde{\boldsymbol{\mu}}, \tilde{\mathcal{K}}, \mathcal{M})$;
- (ii) Draw $\boldsymbol{\theta} \sim p(\boldsymbol{\theta} \mid \mathbf{x}, \mathcal{D}) \propto p(\mathcal{D}, \mathbf{x} \mid \boldsymbol{\theta})p(\boldsymbol{\theta} \mid \boldsymbol{\theta}_0)$,

Omi et al. (2013) used normal distribution with subjective hyperparameters estimated from the prior knowledge as a prior of β . A non-informative constant prior is assumed for that of s^2, ϕ_1, ϕ_2 .

We use Gibbs sampling for sampling from the truncated normal distribution (Geweke 1991, 2005). In R programming language, a package `tmvtnorm` (Wilhelm & Manjunath 2015) can be used to sample from truncated normal distributions. As for sampling of θ , the classical random walk MCMC (Markov Chain Monte Carlo) method (Metropolis et al. 1953) works. For example, in the next section, a random walk MCMC with normal distributions as the proposal distribution is used. By repeating the two steps alternately, obtained $\boldsymbol{\theta}$ becomes samples from posterior of $\boldsymbol{\theta}$. Hyperparameters are estimated as the median of obtained samples. Once samples of \mathbf{x} are obtained, $\boldsymbol{\xi}$ can be estimated by its sample mean since $\boldsymbol{\xi}$ is just the mean of the truncated normal distribution. Therefore, mean and variance of the predictive distribution is also computable with estimated $\boldsymbol{\xi}$.

3 NUMERICAL EXPERIMENTS

We conduct numerical tests under two cases of synthetic observation data in order to illustrate the performance of the proposed method. The two synthetic datasets of elapsed time were generated from the Omori-Utsu and the Gutenberg-Richter laws with the parameters given in Table 1. Assume that the main shock is $M_0 = 6.0$. As for the prior distribution for β , $\mathcal{N}(1.0 \ln(10), 0.2^2)$ is used, but, we put no prior information on τ since the resulting estimates were stable without any prior distributions on τ . The detection function in the two cases is

- (i) $\mu(t) = \frac{1}{1 + 10t} + 1.3$;
- (ii) $\mu(t) = 0.8 \frac{1 + \cos(5\pi t)}{1 + 4t} + 1$,

where the scale parameter s is common within the two cases set to $s = 0.2$. In the first case, $\mu(\cdot)$ is simple and strictly decreasing function, but in the second case, it is more complex. This supposed in

Table 1. The true b and $\tau = (K, c, p)$ values in the Case 1 and 2.

Case	b	$\ln(K)$	p	$\ln(c)$
1	0.9	8.700	1.100	-5.809
2	0.9	8.987	1.100	-5.809

mind that a large aftershock excites many subsequent aftershocks as pointed out in Omi et al. (2013). In Figure 3, the two $\mu(\cdot)$ functions and occurrence rate calculated with synthetic data are shown. We first estimate the predictive distribution of $\mu(\cdot)$ and β , and their credibility with data detected within 3, 6, 12, 24 hours. The number of detected aftershocks are 483, 668, 875, and 1135 at 3, 6, 12, and 24 hours in Case 1; 275, 539, 695, and 925 in Case 2. With the estimated $\hat{\mu}(\cdot)$, $\hat{\beta}$, and \hat{s} , τ is estimated by the method stated in Section 2.3.

Figure 4 shows estimated predictive distribution of $\hat{\mu}(\cdot)$. Mean of the predictive distribution is quite close to the true $\mu(\cdot)$ and inside a region within $3\hat{\sigma}(\cdot)$, where $\hat{\sigma}(\cdot)$ is the estimated standard error of $\hat{\mu}(\cdot)$. The resulting estimates with data (a) $t \leq 3$ does not change so much with (d) $t \leq 24$, which shows robustness of our proposed method for small datasets. It is worth noting that even if mean of the prior distribution (green line) is far from the true one (black dashed line), the predictive distribution can estimate the true $\mu(\cdot)$ considerably well. The estimated $\hat{\beta}$ and $\hat{\tau}$ are also reported in Table 2. The posterior distribution includes the true b -values $b = 0.9$ even data with $t \leq 3$ in both cases, though in Case 2, the estimated b -value is somewhat underestimated, possibly due to the sampling bias. As the elapsed time increases, the center of posterior samples closes to the true value, and the length of the credible interval becomes shorter. Table 2 also shows that comparison of estimated $\hat{\tau}$ with different two methods: (i) proposed method that replaces the detection function $\pi(\cdot)$ with predictive one in eq. (9); (ii) previous method that replaces $\mu(\cdot)$ with estimated $\hat{\mu}(\cdot)$ in eq. (10). The estimates are very similar, but in Case 2, it seems that it fails to estimate p and (or) c values with data $t \leq 12$, while our proposed method gives stable estimates as expected in Section 2.3.

4 REAL DATA ANALYSIS

The proposed method is applied to the real catalog data related to the 2004 Chuetsu earthquake officially released from the Japan Meteorological Agency (JMA). The 2004 Chuetsu earthquake (magnitude $M_0 = 6.8$, epicenter $37^\circ 17' 30''$ N, $138^\circ 52' 00''$ E) occurred in Niigata prefecture, Japan. Figure 5 shows the spatial distribution of aftershocks that occurred within 24 hours from the main shock. The dataset is perfectly the same as used in Omi et al. (2015b), in which the aftershocks occurred in a rectangle area having the lengths four times the Utsu-Seki aftershock zone for latitudinal and longitudinal

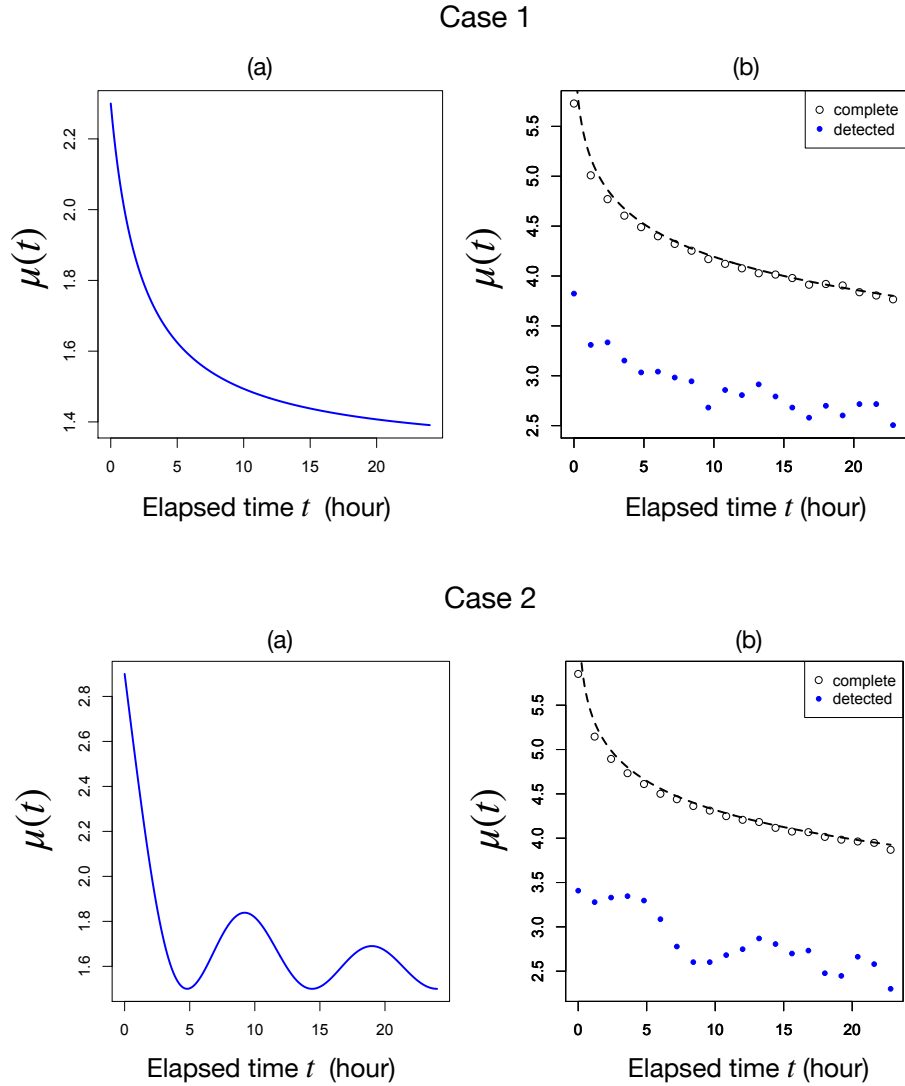


Figure 3. Synthetic data in Case 1. (a) The mean $\mu(t)$ of the true predictive distribution. (b) The occurrence rate of aftershocks $n(t)$. The black solid and blue open circles indicate the complete and detected data, respectively, comparing to the true occurrence rate shown by the dashed line.

directions are selected. The Utsu-Seki aftershock zone is a rectangle region, in which the epicenter is located at the center, having the angle lengths of $2D(M_0)$ for both latitudinal and longitudinal directions, where $D(M_0)$ is the Utsu-Seki aftershock zone length defined using the magnitude of the main shock M_0 as $D(M_0) = 0.01 \times 10^{0.5M_0 - 1.8}$ (Utsu 1969). In the case of the 2004 Chuetsu earthquake, $D(M_0)$ is $23'53''$.

Figure 6 shows the results of applications to the real catalog data. Following the same procedure in the numerical tests in Section 3, the proposed method estimates the mean $\hat{\mu}(\cdot)$ of the predictive distribution with the standard error $\hat{\sigma}(\cdot)$ starting from the prior $\mu_0(\cdot)$, assuming that the data available

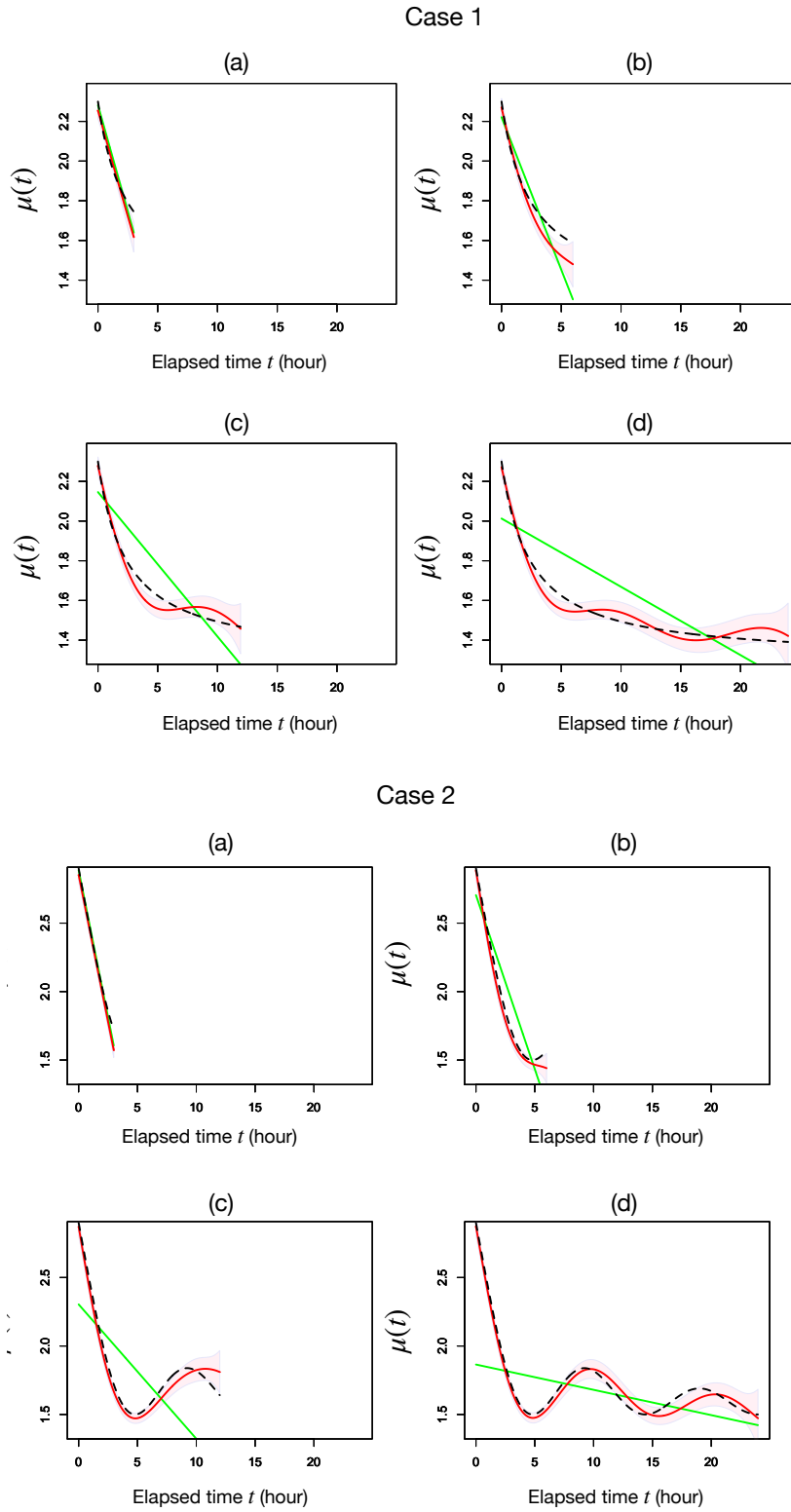


Figure 4. Results of numerical tests to validate the proposed method. The green line indicates the prior of the mean of the predictive distribution $\mu_0(\cdot)$, and the red line indicates the estimated mean $\hat{\mu}(\cdot)$ with the estimation error $\hat{\mu}(\cdot) \pm 3\hat{\sigma}(\cdot)$ shown by the red shaded zone, comparing to the true mean $\mu(\cdot)$ shown by the dashed line, assuming that the data available for (a) 3 hours, (b) 6 hours, (c) 12 hours, and (d) 24 hours from the main shock.

Table 2. Estimates (\pm standard error) of b and $\boldsymbol{\tau} = (K, c, p)^\top$ in the Case 1 and 2 with two methods: (i) proposed method (replacing the detection function with predictive one); (ii) a method used in previous studies (replacing μ function with predictive one (eq. 10))

Case	Data	b	Method (i)			Method (ii)		
			$\ln(K)$	p	$\ln(c)$	$\ln(K)$	p	$\ln(c)$
1	$t \leq 3$	0.846 (± 0.047)	-5.482 (± 0.304)	1.158 (± 0.111)	-5.616 (± 0.437)	-5.476 (± 0.302)	1.156 (± 0.110)	-5.621 (± 0.437)
	$t \leq 6$	0.860 (± 0.043)	-4.902 (± 0.160)	1.155 (± 0.068)	-5.649 (± 0.342)	-4.906 (± 0.160)	1.157 (± 0.068)	-5.644 (± 0.342)
	$t \leq 12$	0.889 (± 0.038)	-4.342 (± 0.094)	1.108 (± 0.045)	-5.844 (± 0.288)	-4.513 (± 0.077)	1.061 (± 0.035)	-6.443 (± 0.310)
	$t \leq 24$	0.901 (± 0.037)	-3.703 (± 0.057)	1.081 (± 0.031)	-5.950 (± 0.262)	-3.701 (± 0.057)	1.081 (± 0.031)	-5.949 (± 0.250)
2	$t \leq 3$	0.846 (± 0.053)	-5.193 (± 0.317)	1.103 (± 0.119)	-5.838 (± 0.574)	-5.192 (± 0.315)	1.102 (± 0.118)	-5.849 (± 0.583)
	$t \leq 6$	0.850 (± 0.044)	-4.320 (± 0.140)	1.022 (± 0.062)	-6.298 (± 0.462)	-4.316 (± 0.142)	1.022 (± 0.063)	-6.303 (± 0.457)
	$t \leq 12$	0.851 (± 0.040)	-3.753 (± 0.104)	1.063 (± 0.053)	-6.052 (± 0.419)	-3.648 (± 0.086)	0.885 (± 0.037)	-7.554 (± 0.492)
	$t \leq 24$	0.859 (± 0.038)	-3.083 (± 0.062)	1.055 (± 0.037)	-6.057 (± 0.350)	-3.077 (± 0.058)	1.052 (± 0.034)	-6.072 (± 0.385)

for 3, 6, 12, and 24 hours from the main shock. The number of aftershocks during each of the elapsed periods is 192, 355, 655, and 1099, respectively. The magnitudes of aftershocks are ranging from 0.8 to 6.6 by the elapsed time of 24 hours.

The $\hat{\mu}(\cdot)$ is found to not simply decrease but turn to increase at $t = 12$ beyond the estimated credible interval $\hat{\mu} + 3\hat{\sigma}$. One possible reason for this may be the fact that a large aftershock occurred at $t = 10.06$ with the magnitude of 4.8. The proposed method can extract such a hidden structure without missing, owing to a stable estimation of $\mu(\cdot)$.

The estimated $\mu(\cdot)$ by Omi et al. (2014) shown in Figure 6 for comparison seems to be unstable when available data were insufficient (Figures 6(a) and 6(b)), which is caused by some approximation methods for the marginal likelihood (supporting information of Omi et al. (2014)), although it is improved when the available data were extended to 24 hours. A similar phenomenon is also seen in Figure 3 in Omi et al. (2013). The proposed method has been improved to make the estimation stable

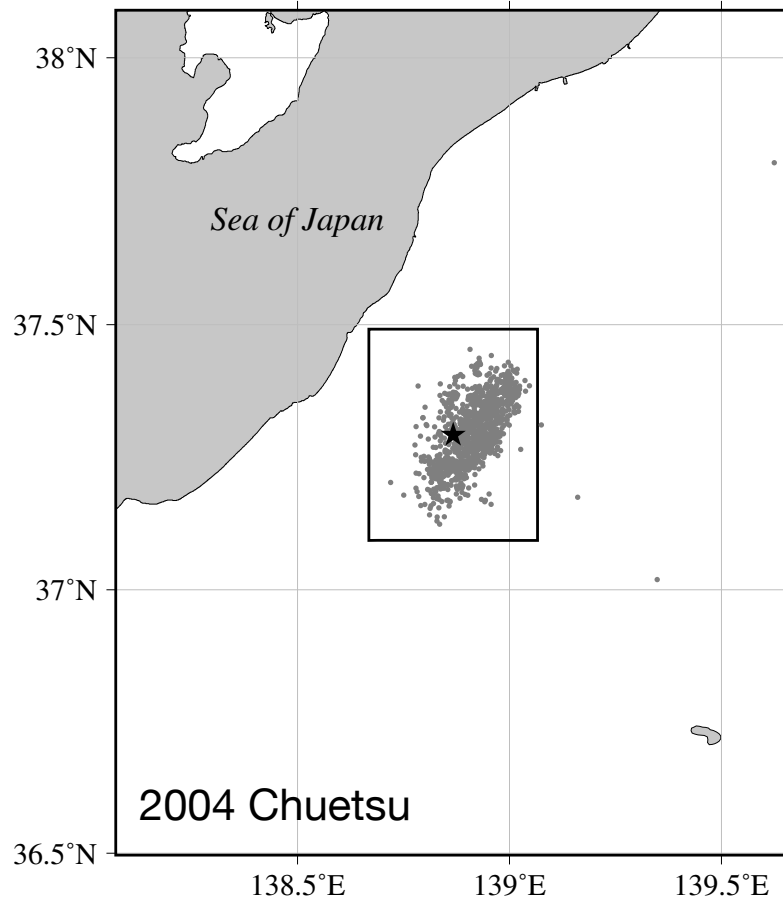


Figure 5. Spatial distribution of aftershocks (circle) within 24 hours from the main shock (star) of the 2004 Chuetsu earthquake officially released by JMA. The small rectangle is the Utsu-Seki aftershock zone, the center of which is the epicenter of the main shock, having the angle lengths of $2D(M_0)$ for both latitudinal and longitudinal directions, where $D(M_0)$ is the Utsu-Seki aftershock zone length.

excluding any approximation for the marginal likelihood (eq. 11). Figure 7(a) shows the estimated predictive detection function (eq. 13) in the case of the 2004 Chuetsu earthquake, and Figure 7(b) plots its cross-sections at the magnitudes $M = 0.8, 1.8, 2.3,$ and 2.8 . These magnitudes correspond to the minimum (0th percentile), 25th percentile, median (50th percentile), and 75th percentile in the catalog data, where q th-percentile is the magnitude below which $q\%$ of all the aftershocks are found. Figure 7(b) indicates that aftershocks with magnitudes larger than 2.3 are completely detected after $t \geq 10$, except $15 < t < 20$ when the detection probability is slightly less than 1 probably due to a large aftershock mentioned above.

Table 2 summarizes mean and standard error of the posterior distribution of b within elapsed time 3, 6, 12, and 24 hours. The 95% credible interval for the b -value computed with the mean and standard error includes the true b -value irrespective to the time available. On the other hand, the estimates of p

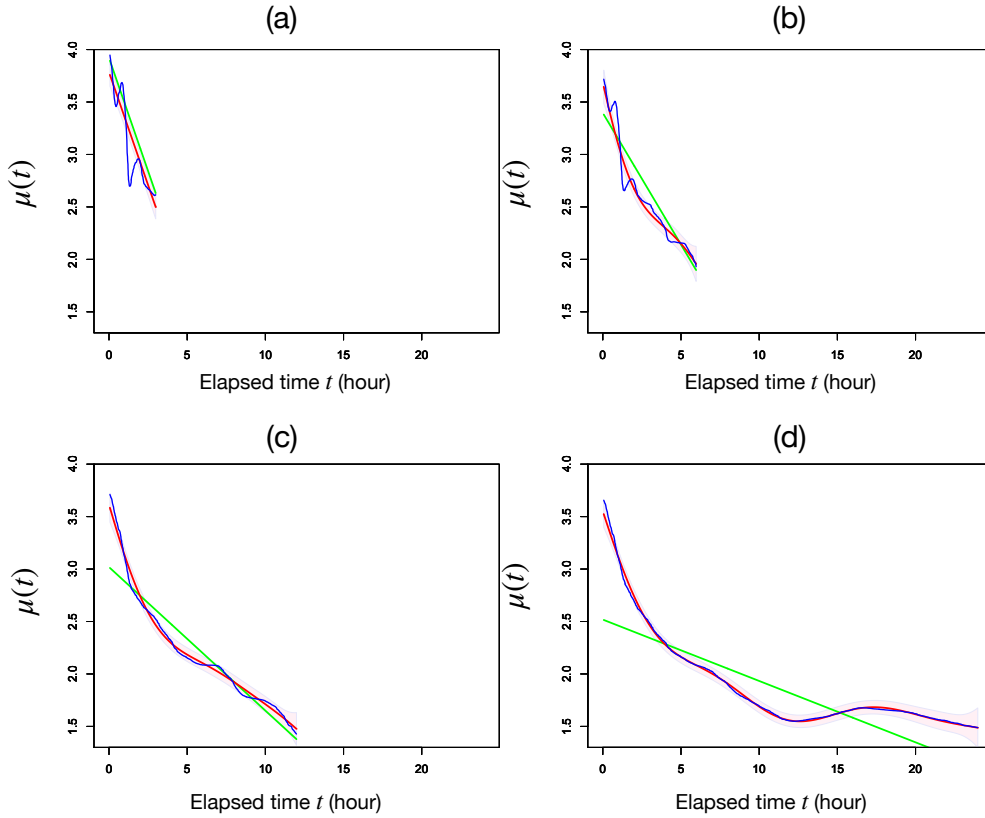


Figure 6. Results of application of our method to the 2004 Chuetsu earthquake. The green line indicates the prior of the mean of the predictive distribution $\mu_0(\cdot)$, and the red line indicates the estimated mean $\hat{\mu}(\cdot)$ with the estimation error $\hat{\mu}(\cdot) \pm 3\hat{\sigma}(\cdot)$ shown by the red shaded zone, comparing to the true mean $\mu(\cdot)$ shown by the dashed line, assuming that the data available for (a) 3 hours, (b) 6 hours, (c) 12 hours, and (d) 24 hours from the main shock.

and c with 24 hours are significantly small compared to the estimates with $t \leq 3, 6, 12$. This indicates our method is successful in detecting the changes of seismic activity due to the large aftershock at $t = 10.06$.

5 CONCLUDING REMARKS

Immediate prediction of seismic activities after the main shock is important to assess hazards for subsequent aftershocks. Contaminations of arriving seismic waves right after the main shock interfere with counting the number of the aftershocks correctly, so that the detected number of the aftershocks is underestimated. This underestimated count of the aftershocks causes distorted estimates for the distribution of the aftershocks or the seismic activities. In order to solve this problem, we introduced a detection function for the aftershocks through GPR to remove the effects of undetected aftershocks. Owing to the nonparametric and Bayesian property of GPR, the proposed detection function has four

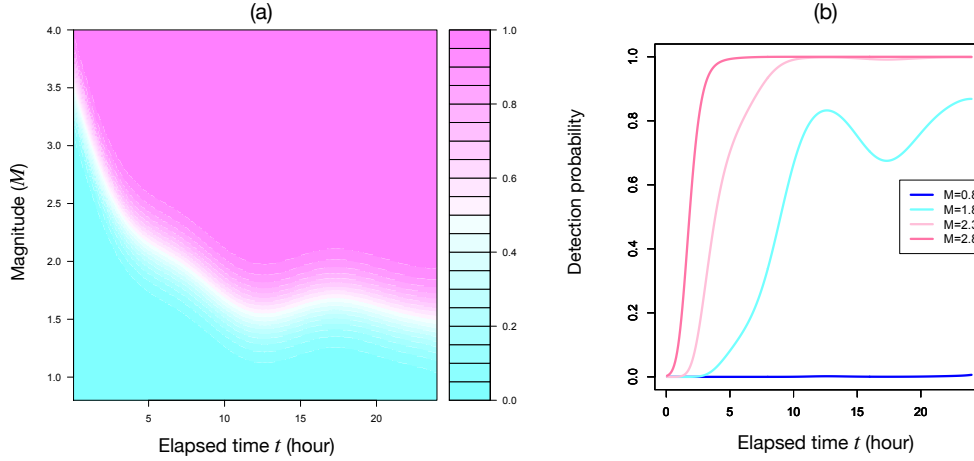


Figure 7. Estimated predictive distribution of detection function $\pi^*(M_1^*, t_1^*)$ with application to method to the 2004 Chuetsu earthquake: (a) predictive distribution of detection probability; (b) predictive distribution of detection probability with fixed magnitude at $M = 0.8, 1.8, 2.3, 2.8$.

advantages superior to the previous methods: (i) the resulting estimates are stable by virtue of a subjective prior; (ii) specification of the detection function is not required; (iii) MCMC sampling is effective to compute the hyperparameters without computation of complicated integration; (iv) credible intervals can be obtained in a natural way.

The limitation of the proposed method is in the assumption on the joint intensity function (eq. 5). It is known that real catalog data should be described by more complicated intensity functions such as represented by Epidemic Type Aftershock Sequence (ETAS) models (Ogata 1988). The proposed method can be extended straightforwardly to ETAS models as done by Omi et al. (2014), which remains as a future work.

Table 3. Estimates (\pm standard error) of b and $\tau = (K, p, c)^\top$ in the Chuetsu earthquake.

Data	b	$\ln(K)$	p	$\ln(c)$
$t \leq 3$	0.787 (± 0.066)	-3.975 (± 0.438)	1.529 (± 0.243)	-3.573 (± 0.478)
$t \leq 6$	0.745 (± 0.051)	-3.129 (± 0.264)	1.484 (± 0.188)	-3.589 (± 0.492)
$t \leq 12$	0.794 (± 0.045)	-2.822 (± 0.117)	1.537 (± 0.123)	-3.509 (± 0.391)
$t \leq 24$	0.779 (± 0.035)	-1.658 (± 0.045)	1.270 (± 0.045)	-3.987 (± 0.362)

ACKNOWLEDGMENTS

This work was mainly supported by Tokyo Metropolitan Resilience Project of National Research Institute for Earth Science and Disaster Resilience (NIED), and partially supported by JST CREST Grant Numbers JPMJCR1763 and JPMJCR1761 of Japan Science and Technology Agency (JST). The key ideas in this study came through the activities of KAKENHI Grant-in-Aids for Early-Career Scientists No. 19K14592, 19K14671, 20K19756, Grant-in-Aids for Scientific Research (B) No. 17H01703, 17H01704, 18H03210, and Grant-in-Aids for Scientific Research (S) No. 19H05662. The travel expense needed to discuss among co-authors was partially supported by ERI JURP 2020-A-05. One of the figures was drawn by using the General Mapping Tools (GMT) developed by (Wessel & Smith 1998).

REFERENCES

- Aki, K., 1965. Maximum likelihood estimate of b in the formula $\log n = a - bm$ and its confidence limits, *Bull. Earthq. Res. Inst. Univ. Tokyo*, **43**, 237–239.
- de G. Matthews, A. G., Rowland, M., Hron, J., Turner, R. E., & Ghahramani, Z., 2018. Gaussian process behaviour in wide deep neural networks, *arXiv preprint: 1804.11271*.
- Genz, A. & Bretz, F., 2009. *Computation of Multivariate Normal and t Probabilities. Lecture Notes in Statistics.*, Heidelberg: Springer.
- Geweke, J. F., 1991. Efficient simulation from the multivariate normal and student- t distributions subject to linear constraints, *Computer Science and Statistics. Proceedings of the 23rd Symposium on the Interface.* Seattle Washington, April 21-24, 1991, 571–578.
- Geweke, J. F., 2005. *Contemporary Bayesian Econometrics and Statistics*, Wiley & Sons.
- Gutenberg, B. & Richter, C. F., 1944. Frequency of earthquakes in california, *Bull. Seism. Soc. Am.*, **34**, 185–188.
- Kagan, Y. Y. & Jackson, D. D., 2000. Probabilistic forecasting of earthquakes, *Geophys. J. Int.*, **143**, 438–453.
- Kuwatani, T., Nagao, H., Ito, S., Okamoto, A., Yoshida, K., & Okudaira, T., 2018. Recovering the past history of natural recording media by bayesian inversion, *Phys. Rev. E*, **98**, 043311.
- Metropolis, N., Rosenbluth, A. W., Rosenbluth, M. N., & Teller, E., 1953. Equations of state calculations by fast computing machine, *J. Chem. Phys.*, **21**, 1087–1091.
- Ogata, Y., 1983. Estimation of the parameters in the modified omori formula for aftershock frequencies by the maximum likelihood procedure, *J. Phys. Earth*, **31**, 115–124.
- Ogata, Y., 1988. Statistical models for earthquake occurrences and residual analysis for point processes, *J. Amer. Statist. Assoc.*, **83**, 29–39.
- Ogata, Y. & Katsura, K., 1993. Analysis of temporal and spatial heterogeneity of magnitude frequency distribution inferred from earthquake catalogs, *Geophys. J. Int.*, **113**, 727–738.

- Ogata, Y. & Katsura, K., 2006. Immediate and updated forecasting of aftershock hazard, *Geophys. Res. Lett.*, **33**, L10305.
- Omi, T., Ogata, Y., Hirata, Y., & Aihara, K., 2013. Forecasting large aftershocks within one day after the main shock, *Sci. Rep.*, **3**, 2218.
- Omi, T., Ogata, Y., Hirata, Y., & Aihara, K., 2014. Estimating the etas model from an early aftershock sequence, *Geophys. Res. Lett.*, **41**, 850–857.
- Omi, T., Ogata, Y., Hirata, Y., & Aihara, K., 2015a. Intermediate-term forecasting of aftershocks from an early aftershock sequence: Bayesian and ensemble forecasting approaches, *J. Geophys. Res.*, **120**, 2561–2578.
- Omi, T., Ogata, Y., Shiomi, K., Enescu, B., Sawazaki, K., & Aihara, K., 2015b. Automatic aftershock forecasting: A test using real-time seismicity data in japan, *Bull. Seismol. Soc. Am.*, **106**, 2450–2458.
- Omori, F., 1894. On the aftershocks of earthquake, *J. Coll. Sci. Imp. Univ. Tokyo*, **7**, 111–200.
- Petersen, K. B. & Petersen, M. S., 2012. The matrix cookbook, Technical report, Technical University of Denmark, 2007. URL <http://www2.imm.dtu.dk/pubdb/p.php?3274>.
- Qin, J., 2017. *Biased Sampling, Over-identified Parameter Problems and Beyond*, Singapore: Springer.
- Rasmussen, C. E., Williams, C. K. I., & Christopher, K. I., 2006. *Gaussian Processes for Machine Learning*, The MIT Press.
- Resenberg, P. A. & Jones, L. M., 1989. Earthquake hazard after a mainshock in california, *Science*, **243**, 1173–1176.
- Resenberg, P. A. & Jones, L. M., 1994. On the estimation of seismic detection thresholds, *Bull. Seismol. Soc. Am.*, **65**, 1631–1642.
- Ringdal, F., 1975. On the estimation of seismic detection thresholds, *Bull. Seism. Soc. Am.*, **65**, 1631–1642.
- Tanner, M. A. & Wong, W. H., 1987. The calculation of posterior distributions by data augmentation, *J. Am. Stat. Assoc.*, **82**, 528–540.
- Utsu, T., 1961. A statistical study on the occurrence of aftershocks, *J. Coll. Sci. Imp. Univ. Tokyo*, **30**, 521–605.
- Utsu, T., 1969. Aftershocks and earthquake statistics (i): Some parameters which characterize an aftershock sequence and their interrelations, *J. Fac. Sci., Hokkaido Univ., Ser. VII (Geophysics)*, **3**, 129–195.
- Utsu, T., 1970. Aftershocks and earthquake statistics (ii)—further investigation of aftershocks and other earthquake sequences based on a new classification of earthquake sequences, *J. Fac. Sci. Hokkaido Univ., Ser.*, **7**, 197–266.
- Vardi, Y., 1982. Nonparametric estimation in presence of length bias, *Ann. Stat.*, **10**, 616–620.
- Vardi, Y., 1985. Empirical distributions in selection bias models, *Ann. Stat.*, **13**, 178–203.
- Wessel, P. & Smith, W. H. F., 1998. New, improved version of generic mapping tools released, *Trans. Am. Geophys. Un.*, **79**, 579.
- Wilhelm, S. & Manjunath, B. G., 2015. *tmvtnorm: Truncated Multivariate Normal and Student t Distribution*, R package version 1.4-10.

APPENDIX A: THEORETICAL RESULTS

In this section, we prove that each the marginal likelihood and the predictive distribution is computed as eq. (11) and eq. (12), respectively. For the proof of eq. (11), a detailed proof is given, but for eq. (12), only a sketch proof is because they are almost same. In the proofs, a formula *sum of two squared forms* (Petersen & Petersen 2012, section 8.1.7) is repeatedly used. The formula says, for any vectors \mathbf{m}_1 and \mathbf{m}_2 , and nonsingular matrices Σ_1 and Σ_2 , it holds that

$$\begin{aligned} & -\frac{1}{2}(\mathbf{x} - \mathbf{m}_1)^\top \Sigma_1^{-1}(\mathbf{x} - \mathbf{m}_1) \\ & -\frac{1}{2}(\mathbf{x} - \mathbf{m}_2)^\top \Sigma_2^{-1}(\mathbf{x} - \mathbf{m}_2) \\ & = -\frac{1}{2}(\mathbf{x} - \mathbf{m}_c)^\top \Sigma_c^{-1}(\mathbf{x} - \mathbf{m}_c) + C, \end{aligned} \tag{A.1}$$

where

$$\begin{aligned} \Sigma_c^{-1} &= \Sigma_1^{-1} + \Sigma_2^{-1} \\ \mathbf{m}_c &= (\Sigma_1^{-1} + \Sigma_2^{-1})^{-1}(\Sigma_1^{-1}\mathbf{m}_1 + \Sigma_2^{-1}\mathbf{m}_2) \\ C &= \frac{1}{2}\mathbf{m}_c^\top \Sigma_c^{-1}\mathbf{m}_c - \frac{1}{2}(\mathbf{m}_1^\top \Sigma_1^{-1}\mathbf{m}_1 + \mathbf{m}_2^\top \Sigma_2^{-1}\mathbf{m}_2). \end{aligned}$$

Proof of Eq. (11). The definition of the marginal likelihood is

$$L(\boldsymbol{\theta}) = p(\beta) \int \prod_{i=1}^n p(M_{1i} | \mu_i; \beta, s^2) p(\boldsymbol{\mu} | \boldsymbol{\mu}_0, \mathcal{K}) d\boldsymbol{\mu}_i, \tag{A.2}$$

where $\boldsymbol{\theta} = (\beta, s^2, \phi_2^2)^\top$, $\boldsymbol{\mu}_0 = (\mu_0(t_{11}), \dots, \mu_0(t_{1n}))^\top$ is mean of the prior distribution, and \mathcal{K} is variance of the prior distribution which is an n by n matrix with (i, j) th element $\mathcal{K}(t_{1i}, t_{1j})$. Hereafter we ignore $p(\beta)$ because it does not have effect on integration. Recall that definition of the conditional distribution of M_1 given $\boldsymbol{\mu}$ is given in eq. (7). It follows from

$$\begin{aligned} & \exp(\beta\mu_i)\Phi(M_{1i}; \mu_i, s^2) \\ &= \frac{\exp(\beta\mu_i)}{\sqrt{2\pi s^2}} \int_{-\infty}^{M_{1i}} \exp\left\{-\frac{(x - \mu_i)^2}{2s^2}\right\} dx \\ &= \frac{\exp(s^2\beta^2/2)}{\sqrt{2\pi s^2}} \int_{-\infty}^{M_{1i}} \exp\left[\beta x - \frac{\{\mu_i - (x + s^2\beta)\}^2}{2s^2}\right] dx \end{aligned}$$

that the conditional distribution can be rewritten as

$$\begin{aligned}
 & \prod_{i=1}^n p(M_{1i} \mid \mu_i; \beta, s^2) \\
 &= \beta^n \exp \left\{ -\beta \sum_{i=1}^n M_{1i} - \frac{n}{2} \beta^2 s^2 \right\} \prod_{i=1}^n \exp(\beta \mu_i) \Phi(M_{1i}; \mu_i, s^2) \\
 &= \frac{\beta^n \exp(-\beta \sum_{i=1}^n M_{1i})}{\sqrt{(2\pi)^n |\Sigma|}} \int_{\mathbf{x} \in \mathcal{M}} \exp(\beta \mathbf{1}^\top \mathbf{x}) \\
 & \quad \times \exp \left[-\frac{1}{2} \{ \boldsymbol{\mu} - (\mathbf{x} + \beta \Sigma \mathbf{1}) \}^\top \Sigma^{-1} \{ \boldsymbol{\mu} - (\mathbf{x} + \beta \Sigma \mathbf{1}) \} \right] d\mathbf{x},
 \end{aligned}$$

where $\Sigma = s^2 I_n$, I_n is n by n identity matrix, and $\mathcal{M} = \otimes_{i=1}^n \{x_i \leq M_{1i}\}$. Letting $\mathbf{m}_1 = \mathbf{x} + \beta \Sigma \mathbf{1}$, $\mathbf{m}_2 = \boldsymbol{\mu}_0$, $\Sigma_1 = \Sigma$, and $\Sigma_2 = \mathcal{K}$ with the formula (eq. A.1), leads to

$$\begin{aligned}
 & L(\boldsymbol{\theta}) \\
 &= \frac{\beta^n \exp(-\beta \sum_{i=1}^n M_{1i})}{\sqrt{(2\pi)^n |\Sigma|} \sqrt{(2\pi)^n |\mathcal{K}|}} \int_{\mathcal{M}} \exp(\beta \mathbf{1}^\top \mathbf{x}) \\
 & \quad \times \int \exp \left\{ -\frac{1}{2} (\boldsymbol{\mu} - \mathbf{m}_1)^\top \Sigma_1^{-1} (\boldsymbol{\mu} - \mathbf{m}_1) \right\} \\
 & \quad \times \int \exp \left\{ -\frac{1}{2} (\boldsymbol{\mu} - \mathbf{m}_2)^\top \Sigma_2^{-1} (\boldsymbol{\mu} - \mathbf{m}_2) \right\} d\boldsymbol{\mu} d\mathbf{x} \\
 &= \frac{\beta^n \exp(-\beta \sum_{i=1}^n M_{1i})}{(2\pi)^n \sqrt{|\Sigma| |\mathcal{K}|}} \\
 & \quad \times \int_{\mathcal{M}} \exp(\beta \mathbf{1}^\top \mathbf{x}) \sqrt{(2\pi)^n |\Sigma_c|} \exp(C) d\mathbf{x}.
 \end{aligned}$$

Next, we compute m_c , Σ_c , and C in the formula. It follows from the standard argument in linear algebra that

$$\begin{aligned}
 \Sigma_c &= (\mathcal{K}^{-1} + \Sigma^{-1})^{-1} = \mathcal{K} \tilde{\mathcal{K}}^{-1} \Sigma, \\
 \mathbf{m}_c &= \Sigma_c \{ \Sigma^{-1} (\mathbf{x} + \beta \Sigma \mathbf{1}) + \mathcal{K}^{-1} \boldsymbol{\mu}_0 \}, \\
 C &= -\frac{1}{2} \boldsymbol{\mu}_0^\top \tilde{\mathcal{K}}^{-1} \boldsymbol{\mu}_0 - \frac{1}{2} (\mathbf{x} + \beta \Sigma \mathbf{1})^\top \tilde{\mathcal{K}}^{-1} (\mathbf{x} + \beta \Sigma \mathbf{1}) \\
 & \quad + \boldsymbol{\mu}_0^\top (\mathcal{K} + \Sigma)^{-1} (\mathbf{x} + \beta \Sigma \mathbf{1}),
 \end{aligned}$$

where $\tilde{\mathcal{K}} = \mathcal{K} + \Sigma$. Rearranging the integrand so that it becomes a quadratic form of \mathbf{x} , we have

$$\begin{aligned}
 & L(\boldsymbol{\theta}) \\
 &= \frac{\beta^n}{\sqrt{(2\pi)^n |\tilde{\mathcal{K}}|}} \exp \left\{ -\beta \sum_{i=1}^n (M_{1i} - \mu_{0i}) - \frac{\beta^2}{2} \mathbf{1}^\top (\Sigma - \mathcal{K}) \mathbf{1} \right\} \\
 & \quad \times \int_{\mathcal{M}} \exp \left\{ -\frac{1}{2} (\mathbf{x} - \tilde{\boldsymbol{\mu}})^\top \tilde{\mathcal{K}}^{-1} (\mathbf{x} - \tilde{\boldsymbol{\mu}}) \right\} d\mathbf{x},
 \end{aligned}$$

where $\tilde{\boldsymbol{\mu}} = \boldsymbol{\mu}_0 + \beta \mathcal{K} \mathbf{1}$. This is the desired conclusion.

Proof of Eq. (12). Let t_1^* be any data point may not be in the dataset. What we need to compute is

$$\begin{aligned} & p(\mu^* | t_1^*, \mathcal{D}) \\ &= \int p(\mu^* | t_1^*, \boldsymbol{\mu}, \mathbf{t}_1) p(\boldsymbol{\mu} | \mathbf{t}_1, \mathbf{M}_1) d\boldsymbol{\mu} \\ &= \frac{\int p(\mu^* | t_1^*, \boldsymbol{\mu}, \mathbf{t}_1) p(\mathbf{M}_1 | \boldsymbol{\mu}) p(\boldsymbol{\mu} | \mathbf{t}_1) d\boldsymbol{\mu}}{\int p(\mathbf{M}_1 | \boldsymbol{\mu}) p(\boldsymbol{\mu} | \mathbf{t}_1) d\boldsymbol{\mu}}. \end{aligned}$$

Here, denominator of the predictive distribution is exactly the same as the marginal likelihood which is already computed. Hence it remains to show the numerator becomes

$$\begin{aligned} & \beta^n \exp \left\{ -\beta \sum_{i=1}^n (M_{1i} - \mu_{0,i}) - \frac{1}{2} \beta^2 \left(ns^2 - \sum_{i,j} \mathcal{K}_{i,j} \right) \right\} \\ & \times \int_{\mathcal{M}} \mathcal{N}(\mu^*; D(\mathbf{x}), \tau^2) \mathcal{N}(\mathbf{x}; \tilde{\boldsymbol{\mu}}, \tilde{K}) d\mathbf{x}. \end{aligned}$$

It is computed by using the formula (eq. A.1) with respect to $\boldsymbol{\mu}$ with some tedious calculus.

Proof of Eq. (13). It follows from the result of eq. (12) that

$$\begin{aligned} & P(\delta = 1 | M_1^*, t_1^*, \mathcal{D}) \\ &= \int P(\delta = 1 | M_1^*, \mu^*, \mathcal{D}) p(\mu^* | t_1^*, \mathcal{D}) d\mu^* \\ &= \int_{-\infty}^{\infty} \int_{-\infty}^M \mathcal{N}(z; \mu^*, s^2) \\ & \quad \times \frac{\int_{\mathcal{M}} \mathcal{N}(\mu^*; D^*(\mathbf{x}), (\tau^*)^2) \mathcal{N}(\mathbf{x}; \tilde{\boldsymbol{\mu}}, \tilde{K}) d\mathbf{x}}{\int_{\mathcal{M}} \mathcal{N}(\mathbf{x}; \tilde{\boldsymbol{\mu}}, \tilde{K}) d\mathbf{x}} d\mu^* \\ &= \int_{-\infty}^M \frac{\int_{\mathcal{M}} \mathcal{N}(z; D^*(\mathbf{x}), s^2 + (\tau^*)^2) \mathcal{N}(\mathbf{x}; \tilde{\boldsymbol{\mu}}, \tilde{K}) d\mathbf{x}}{\int_{\mathcal{M}} \mathcal{N}(\mathbf{x}; \tilde{\boldsymbol{\mu}}, \tilde{K}) d\mathbf{x}} dz \\ &= \mathbb{E}_{\text{trunc}} \left\{ \Psi \left(\frac{M_1^* - D^*(\mathbf{X})}{\sqrt{s^2 + (\tau^*)^2}} \right) \right\}. \end{aligned}$$

Proof of Eq. (14). By using the Fubini's theorem, we have

$$\begin{aligned}
 & \nu^*(t; \tau, \beta, s) \\
 &= \int_{-\infty}^{\infty} \lambda(t, M; \tau, \beta) \mathbb{E}_{\text{trunc}} \left\{ \Psi \left(\frac{M - D^*(\mathbf{X})}{\sqrt{s^2 + (\tau^*)^2}} \right) \right\} dM \\
 &= \frac{K}{(t+c)^p} \int_{-\infty}^{\infty} \beta e^{-\beta(M-M_0)} \\
 &\quad \times \frac{\int_{-\infty}^M \mathcal{N}(z; D^*(\mathbf{x}), s^2 + (\tau^*)^2) dz \int_{\mathcal{M}} \mathcal{N}(\mathbf{x}; \tilde{\mu}, \tilde{K}) d\mathbf{x}}{\int_{\mathcal{M}} \mathcal{N}(\mathbf{x}; \tilde{\mu}, \tilde{K}) d\mathbf{x}} dM \\
 &= \frac{K}{(t+c)^p} \int_{-\infty}^{\infty} \int_z^{\infty} \beta e^{-\beta(M-M_0)} dM \\
 &\quad \times \frac{\mathcal{N}(z; D^*(\mathbf{x}), s^2 + (\tau^*)^2) \int_{\mathcal{M}} \mathcal{N}(\mathbf{x}; \tilde{\mu}, \tilde{K}) d\mathbf{x}}{\int_{\mathcal{M}} \mathcal{N}(\mathbf{x}; \tilde{\mu}, \tilde{K}) d\mathbf{x}} dz \\
 &= \frac{K}{(t+c)^p} \mathbb{E}_{\text{trunc}} \left[\exp \left\{ -\beta(D^*(\mathbf{x}) - M_0) + \frac{1}{2} \beta^2 (s^2 + (\tau^*)^2) \right\} \right],
 \end{aligned}$$

as desired.